# Subsurface structure of interannual temperature anomalies in the Australian sector of the Southern Ocean

Serguei Sokolov and Stephen R. Rintoul

Commonwealth Scientific and Industrial Research Organization, Marine Research and Antarctic Cooperative Research Centre, Hobart, Tasmania, Australia

[1]   A 7 year time series of austral summer expendable bathythermograph (XBT) sections between Tasmania and Antarctica is used to describe the subsurface structure of Southern Ocean interannual temperature anomalies. Comparison of the discontinuous XBT record with a continuous (weekly average) satellite-based SST data set confirms that the XBT sampling is adequate to resolve interannual variability. Significant correlations are found between changes in surface and subsurface temperature along much of the section. In the Subantarctic zone, surface and subsurface changes are coherent because deep convection in winter homogenizes the upper 600 m, and the summer mixed layer temperature reflects the preconditioning of the previous winter. At other latitudes the regions of high correlation generally extend well beyond the depth of direct atmospheric influence (i.e., the depth of the winter mixed layer). Negative (positive) temperature anomalies at interannual timescales are coherent with poleward (equatorward) displacements of fronts. The simplest explanation for the correspondence between deep, vertically coherent temperature anomalies and the location of ACC fronts is that the observed features reflect meridional shifts of temperature gradients associated with the fronts. The link between temperature anomalies and front displacements suggests Southern Ocean sea surface temperature (SST) anomalies primarily reflect a dynamical response of the ocean to wind or other forcing rather than surface-trapped features produced by anomalous air-sea heat flux. The XBT record contains both interannual and longer (unresolved) period signals, which cannot be isolated in the short discontinuous XBT time series. Spectral analysis of the 17 year SST data set reveals roughly equal variability in 2–7 year and >7 year bands.   *INDEX TERMS:* 4207 Oceanography: General: Arctic and Antarctic oceanography; 4215 Oceanography: General: Climate and interannual variability (3309); 4528 Oceanography: Physical: Fronts and jets; 4572 Oceanography: Physical: Upper ocean processes; *KEYWORDS:* Antarctic circumpolar wave, Southern Ocean, Antarctic circumpolar current, interannual variability, decadal variability, sea surface temperature anomaly

## 1.   Introduction

[2]   In recent years, the availability of relatively long data sets has revealed variability in the atmosphere-ocean-sea ice system at high southern latitudes at a variety of temporal and spatial scales. Examples include the decadal variability of the semiannual oscillation in mean sea level pressure [*Meehl et al.*, 1998], the southern annular mode or Antarctic Oscillation [*Thompson et al.*, 2000], the Antarctic Dipole [*Yuan and Martinson*, 2000], and changes in Southern Ocean water masses [e.g., *Bindoff and McDougall*, 2000; *Gille*, 2002].

[3]   The Antarctic Circumpolar Wave (ACW) [*White and Peterson*, 1996] has attracted particular interest. The ACW is a zonal wave number two pattern of anomalies in sea surface temperature (SST), sea ice extent, sea level pressure, and meridional wind stress that propagates around Antarctica with a period of about eight years. Various hypotheses have been proposed to explain how the ACW is initiated and maintained. Some authors maintain the ACW is generated in response to atmospheric teleconnections driven by SST anomalies in the tropical Pacific [*Peterson and White*, 1998; *Baines and Cai*, 2000], while others conclude the ACW results from an instability of the coupled atmosphere-ocean system which is independent of tropical forcing [*Qiu and Jin*, 1997; *Goodman and Marshall*, 1999]. *White et al.* [1998] and *Talley* [1999] present simple coupled ocean-atmosphere models which explain many of the characteristics of the ACW. In particular, *White et al.* [1998] show that the modeled ACW propagates too slowly and dissipates when no coupling between the ocean and atmosphere is allowed. However, other studies suggest the ACW reflects a

passive ocean response to atmospheric forcing, with no feedback from ocean to atmosphere [*Weisse et al.*, 1999; *Christoph et al.*, 1998; *Bonekamp et al.*, 1999]. While the dynamics of the ACW are of interest in their own right, the ACW has also attracted attention because the anomalies appear to be related to rainfall variability in southern hemisphere continents, and so may form the basis of a statistical climate prediction system [*White and Cherry*, 1998; *White*, 2000].

[4] The description of Southern Ocean variability has relied heavily on satellite measurements of SST, which now extend over almost two decades. Measurements of subsurface temperature are comparatively scarce. As a result, the dynamics and impacts of variability of the atmosphere-ocean-ice system in the Southern Ocean region remain obscure. In particular, the lack of subsurface data means that we have not been able to determine if the ocean response is limited to the surface layer or if the ocean temperature anomalies extend to depth. The former might be expected if the ocean is responding directly to changes in air-sea heat flux; the latter might reflect, for example, a dynamical response to changes in wind stress curl through the vorticity balance. Most studies to date have modeled the ocean expression of the ACW as SST anomalies advected eastward around the Southern Ocean by the Antarctic Circumpolar Current. If the temperature anomalies penetrate to depth, different physics are likely required to explain the ACW.

[5] Previous studies of subsurface temperature variability in the Southern Ocean have been limited to particular locations or to a few repeat sections occupied over a number of years [e.g., *Aoki*, 1997]. Here we use a 7 year time series of XBT sections south of Australia to examine the subsurface structure of Southern Ocean temperature anomalies. While our data set is limited to a short period at a single longitude, it is the first with sufficient temporal and spatial resolution to begin to examine interannual temperature anomalies in the upper 800 m across the full width of the Southern Ocean. We find significant correlations between surface and subsurface temperature variability and relate the vertically coherent changes to displacements of the major Southern Ocean fronts. We conclude that Southern Ocean interannual temperature anomalies likely reflect a dynamical response to changes in wind-forcing rather than air-sea heat flux anomalies.

## 2. Data

[6] XBT data were collected along a repeat section between Tasmania and Antarctica near 145°E (Figure 1) as part of the joint Australia-France-USA SURVOSTRAL experiment [*Rintoul et al.*, 1997]. The section is typically occupied six times each season between late winter/early spring (October) and autumn (March). A total of 45 sections have been obtained between 1992 and 1999. The SURVOSTRAL program is conducted from the French Antarctic supply ship *Astrolabe*, and the sampling schedule is set by requirements to resupply the Antarctic base *Dumont d'Urville*. The typical station spacing is 37 km, with 19 km spacing across the ACC fronts. Temperature is measured to 800 m. Extreme weather occasionally causes
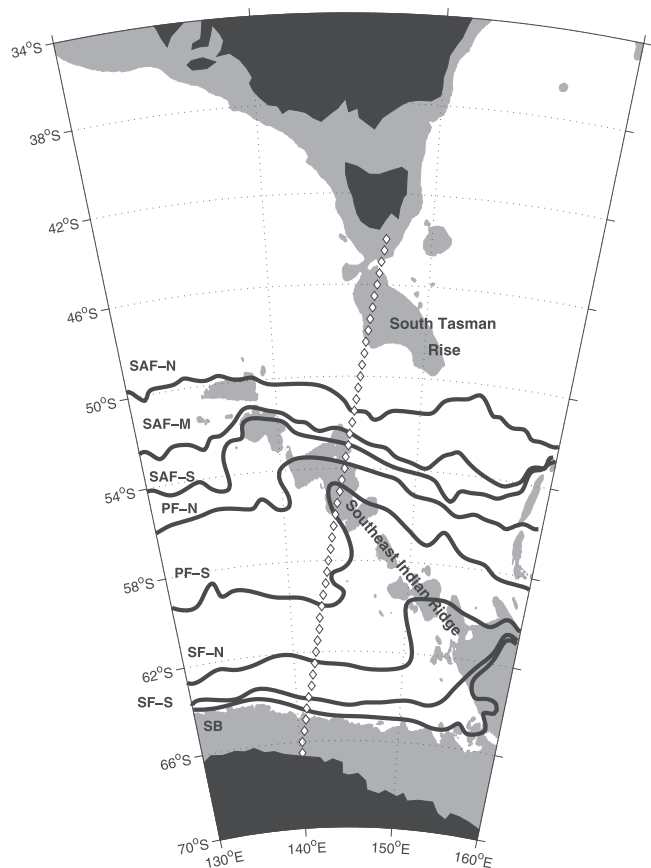


**Figure 1.** Cruise track of *Astrolabe*, the SURVOSTRAL section (diamonds). Depths less than 3500 m are indicated by light shading. Modal path of the major fronts in the Australian sector are estimated from altimetry data for the period between 1992 and 2000 [*Sokolov and Rintoul*, 2002]. SAF, Subantarctic Front; PF, Polar Front; SF, southern ACC front; SB, southern boundary of the ACC. Northern, middle, and southern branches of each front, where applicable, are indicated by −N, −M, and −S.

gaps in the sections, and some of the sections deviate significantly from the mean cruise track. To reduce error owing to differences in spatial sampling, data from seven sections that deviated from the mean cruise track by more than 1° of longitude were not used.

[7] The XBT time series is both short and discontinuous. To test whether the temporal sampling is adequate to describe the variability on interannual timescales, we compare the surface temperatures measured by XBTs to weekly mean SST from *Reynolds and Marsico* [1993], which is largely based on satellite data. Our focus here is on interannual variability. Higher frequency variability was removed from the XBT temperatures by averaging together data from each austral summer; the data were also averaged in latitude bands. To derive the interannual signal from weekly SST data, the data were bandpassed with a 2 to 7 year period admittance window, as in the work of *White et al.* [1998]. For the period where the two time series overlap, the agreement is very good (see below).

[8] Interannual and longer period signals cannot be separated in the short XBT record. We therefore use the longer

satellite-derived SST data set to examine the SST variability in different frequency bands.

## 3.   Results

[9]   To orient the reader in the following discussion of the relationship between temperature anomalies and the location of fronts, Figure 1 shows the modal path of the main fronts of the Antarctic Circumpolar Current (ACC) south of Tasmania [from *Sokolov and Rintoul*, 2002]. Sokolov and Rintoul use repeat hydrographic sections to demonstrate that the Subantarctic Front (SAF), Polar Front (PF) and southern ACC front (SF) all consist of multiple branches in this region. They further showed that each branch coincides with a narrow range of surface dynamic height, allowing the fronts to be identified in maps of sea surface height (SSH) prepared by adding satellite-measured height anomalies to a mean field [from *Olbers et al.*, 1992]. The paths in Figure 1 represent the modal position of each frontal branch over the period between 1992 and 2000. The Subtropical Front (STF) is not shown in Figure 1 because its signature in SSH is weak and it cannot be traced in this way. Repeat XBT and hydrographic sections show the STF is found between 45°S and 47°S, in the deep saddle between Tasmania and the South Tasman Rise [*Rintoul et al.*, 1997; *Sokolov Rintoul*, 2002]. In common with meridional sections across the Southern Ocean at other longitudes, temperature changes across the fronts make the dominant contribution to north-south changes in the thermal field throughout the full ocean depth (as illustrated below).

### 3.1.   Temporal Evolution of SST Anomalies and Adequacy of Sampling

[10]   The irregular sampling of the XBT data may alias variability at unresolved frequencies. To verify the XBT sampling is sufficient to capture the interannual signals of interest, we compare three filtered records of SST: XBT measurements of SST averaged in 1° latitude bins for each austral summer season ($SST_{XBT}$), Reynolds SST sampled at the time of each XBT section and averaged in the same latitude bins ($SST_{summer}$), and low-pass filtering of the complete annual cycle of Reynolds SST to retain signals with a period longer than 2 years ($SST_{cont}$).

[11]   XBT and satellite measurements of SST result in a similar distribution of mean temperature as a function of latitude, when averaged in a similar way (Figure 2a). The summer-average curves are biased high (by about 1.2°C) relative to the low-pass filtered continuous satellite SST data, as expected since the latter includes winter data. The distribution of SST gradient is also similar between $SST_{XBT}$ and $SST_{summer}$, with maximum gradients near the fronts, but the satellite data underestimates the strong gradients near the SAF (50° to 53°S, Figure 2b). The weaker gradients in the Reynolds SST likely reflect spatial smoothing of the high gradient regions in the mapping of the satellite data. This is supported by Figure 2c, which shows how the differences between the three SST records depend on latitude. The greatest differences between $SST_{XBT}$ and $SST_{summer}$ are found between 50°S and 55°S, in the vicinity of the SAF and PF-N. Differences greater than 0.2°C also occur near the STF at 46°S, and south of 63°S, where the quality of the satellite data is poor owing to ice cover. The

RMS difference is about 0.3°C. The hypothesis that the Reynolds SST data are overly smoothed is further supported by the fact that a 9 km resolution satellite SST product [*Walker and Wilkin*, 1998] shows a similar offset from the Reynolds SST data near the SAF (Figure 2c). Figure 2d shows the number of XBT casts in each 1° latitude bin average, indicating the poor sampling in the 1992–1993 austral summer season.

[12]   Figure 2 demonstrates that the XBT and satellite measurements of SST are consistent in terms of mean temperature and gradient, with the exception of a bias owing to excessive smoothing of the SAF in the satellite data. We now compare the interannual variability signal in each of the three filtered time series, averaged in 2° latitude bins (Figure 3). $SST_{XBT}$ (thin solid line) and $SST_{summer}$ (thick solid line) generally track each other closely across the entire section. Although the filtered continuous record is offset from those based on summer data only, $SST_{cont}$ (thick dashed line) shows similar year-to-year changes to the other two records.

[13]   The meridional structure of the interannual variability in SST is more clearly illustrated in the time-latitude plot of low-passed SST anomalies in Figure 4. The pattern of positive and negative anomalies from the two records is very similar across the width of the Southern Ocean. The major discrepancies occur in 1993, when few XBT sections were occupied at the start of the program. Interannual anomalies derived from continuous satellite SST are smaller in amplitude and smoother relative to the signal derived from XBT measurements, reflecting smoothing of high gradient regions in the satellite SST maps. We conclude from this comparison that the XBT sampling is adequate to capture the interannual variability in SST.

### 3.2.   Subsurface Structure of Southern Ocean Temperature Anomalies

[14]   The year-to-year variability in summer average temperatures at six depths is shown in Figure 5 for selected latitudes (the surface temperature line is repeated from Figure 3). The summer mixed layer is generally about 100 m thick and so we expect temperature anomalies at 50 m to track those at the sea surface, as observed. At 63°S, the summer mixed layer is shallower than 50 m and temperature at 0 m and 50 m is uncorrelated. At some latitudes, high correlation between surface and subsurface temperature extends well below the mixed layer. For example, at 47°S the interannual variations are similar from 0 m to at least 200 m depth. At 49°S temperature changes are well-correlated between 200 m and 600 m depth, but are not correlated with changes in the mixed layer. Temperature changes are coherent at all depths from 0–600 m at 51°S, with high temperatures in 1993 and 1999 and a minimum in 1997. South of 55°S, the interannual variability is very weak at 400 m and 600 m depth and the surface and subsurface layers are not correlated.

[15]   Figure 5 indicates that changes in surface temperature are reflected at depth in some, but not all, parts of the section. The connection between surface and subsurface temperature anomalies is more clearly illustrated in Figure 6. The upper panel shows the mean temperature in the upper 700 m and the location of the major fronts. The lower panel shows the correlation between surface and subsurface
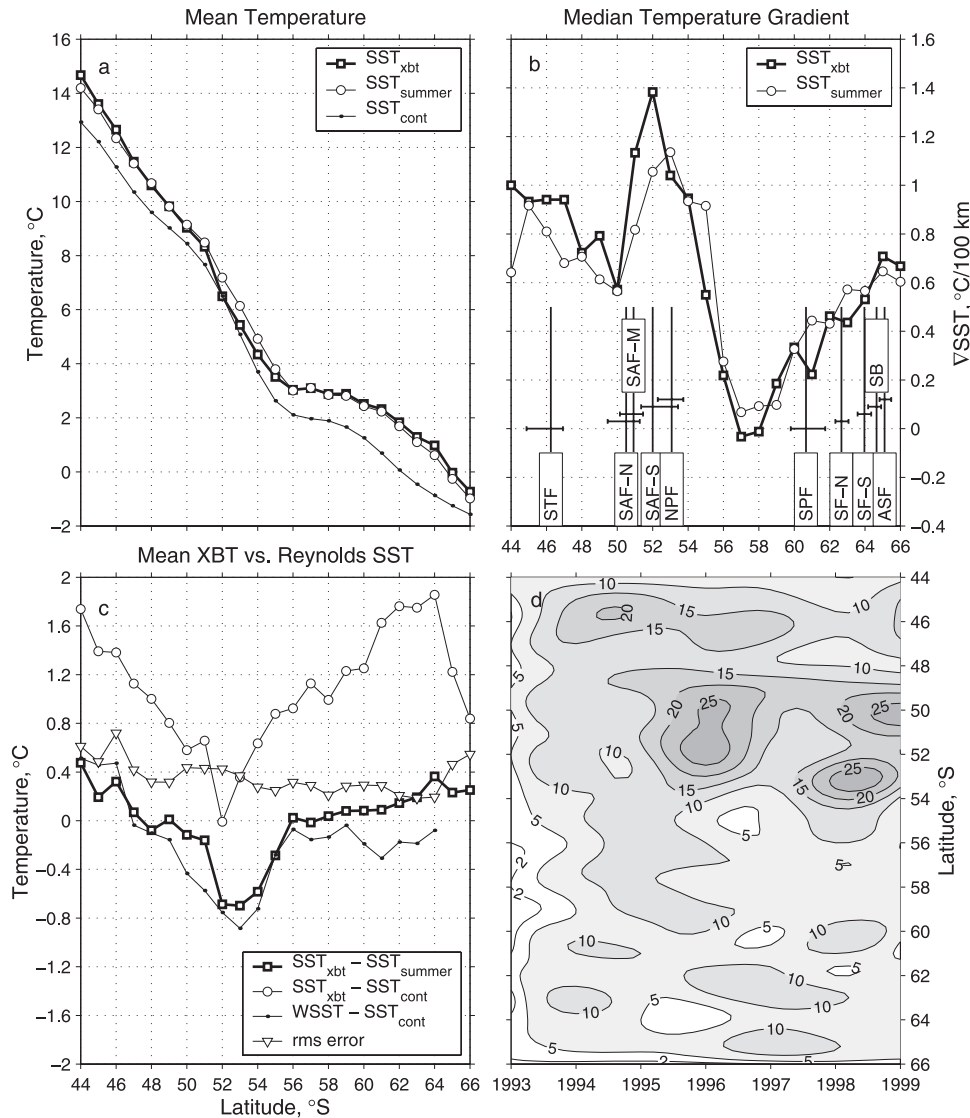
**Figure 2.** Distribution of (a) mean temperature and (b) median temperature gradients derived from XBT and satellite SST measurements. (c) Mean XBT estimates (SST$_{xbt}$) are compared with those derived from continues Reynolds SST data (SST$_{cont}$), averaged in a similar to XBT way Reynolds SST data (SST$_{summer}$) and high-resolution SST data mapped on 9-km grid (WSST). (d) Number of XBT data averaged in 1° latitude bands each austral summer is shown. Also, mean major front locations derived from individual XBT sections are given in Figure 2b. Latitudinal ranges of individual fronts' locations are indicated by horizontal bars.

temperature variability over the 7 year XBT record. Correlations were calculated between the SST and deep XBT temperatures on a 1° latitude grid with 10 dbar vertical resolution. Regions with correlations higher than the 80% confidence level are indicated by shading.

[16] Temperature changes at and north of the STF, near 46°S, are highly correlated from the sea surface down to 400 m depth which corresponds to the vertical extent of the STF. The interannual temperature variations extend even deeper in the water column in the Subantarctic zone (SAZ) south of the STF (46–48°S), within the pool of Subantarctic Mode Water (SAMW). Surface and subsurface temperature changes are also vertically coherent throughout the upper ocean in the vicinity of the SAF and PF (50 to 54°S).

[17] The only latitude band on the northern half of the section where the subsurface changes in temperature do not track those at the surface is the part of the SAZ between 48 and 50°S. In this band, the interannual variability is dominated by the presence or absence of a cold core ring or meander pinched off from the SAF. Cold core features are often, but not always, observed in this location: of 32 sections with sufficient resolution to say whether the cold core feature is present, 28 (88%) have at least a weak eddy/meander; 19 of the 32 (59%) have a strong feature [*Rintoul et al.*, 2002; *Sokolov and Rintoul*, 2002]. The strong temperature and salinity anomalies associated with the eddy extend throughout the water column, but are rapidly removed by mixing and air-sea exchange above
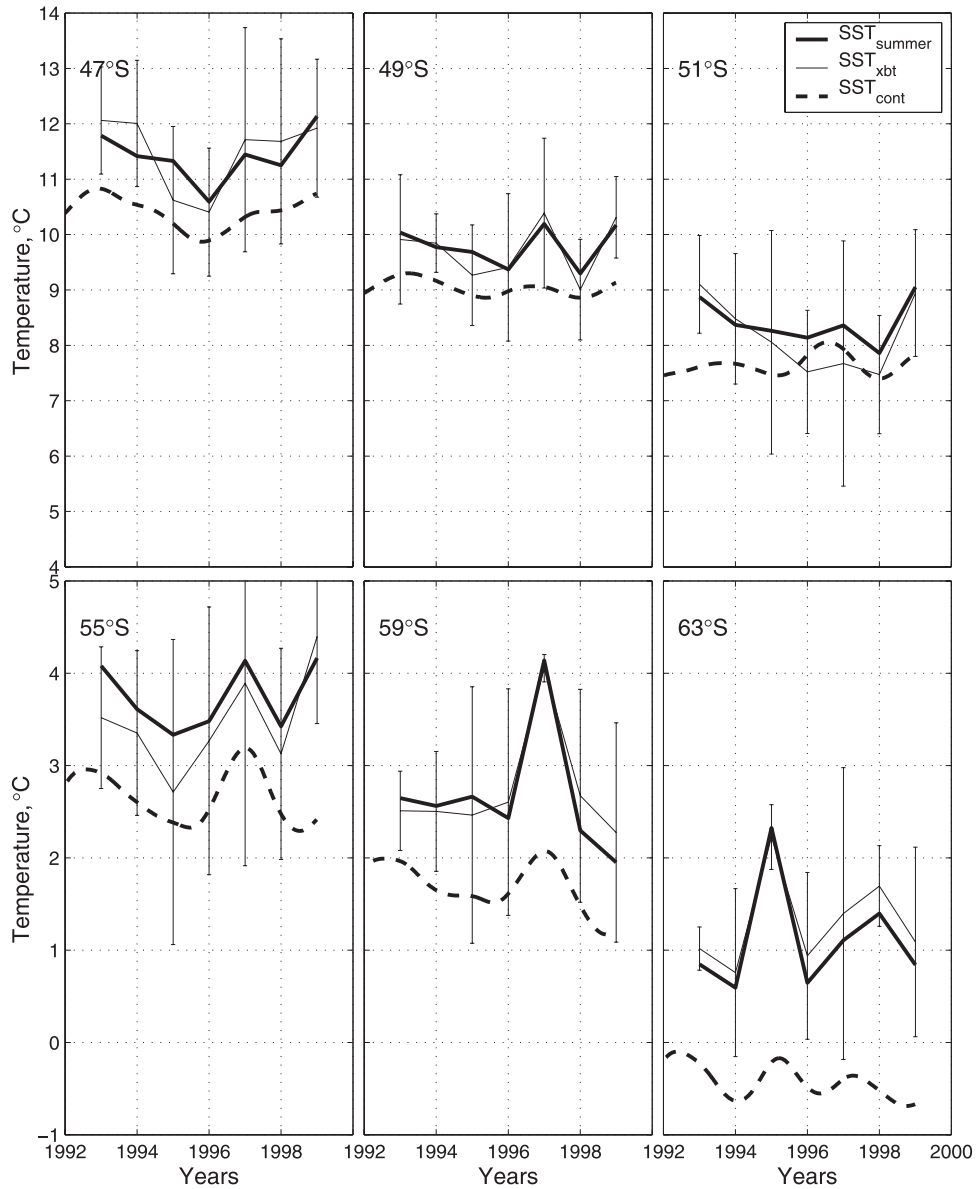
**Figure 3.** Interannual temperature changes across the SURVOSTRAL section. Casts within a 2° latitude band have been averaged for each austral summer. XBT measurements of SST (SST$_{xbt}$, thin solid line) can be compared to the continuous SST data retaining longer than 2 year variations (SST$_{cont}$, thick dashed line), and to the austral summer averaged SST (SST$_{summer}$, thick solid line). Standard deviations of sea surface XBT temperature estimated for each austral summer are indicated by vertical bars.

the seasonal thermocline [*Rintoul et al.*, 1997]. Hence changes in summer mixed layer temperature are not correlated with deeper temperature changes in this latitude band.

[18] South of the northern branch of the PF at 54°S, the vertical correlation structure becomes more complex. Interannual changes in SST are generally coherent with subsurface temperature changes only within the summer mixed layer (upper 50 m), and do not appear in the underlying remnant winter mixed layer (or WW) which lies between 50 and 250 m. Although interannual temperature changes in the WW are independent from those in the surface layer, they are horizontally coherent between 55°S and 63°S (not shown).

[19] The lack of correlation between temperature variations at the surface and below the WW layer reflects the temperature distribution at these depths. The Upper Circumpolar Deep Water (UCDW) coincides with the subsurface temperature maximum layer below the WW. Within the UCDW, horizontal and vertical temperature gradients are very small. The nearly isothermal nature of the UCDW means that meridional or vertical translations result in little change in temperature. As a result, interannual variations in the UCDW do not exceed 0.05°C.

[20] Temperature gradients increase at greater depth (near the transition from UCDW to Lower Circumpolar Deep Water (LCDW), which shoals from about 700 m at 56°S to 200 m at 64°S). Meridional shifts of the temperature field at these depths therefore result in larger temperature changes and significant correlations with surface anomalies at the front positions. The regions of high correlation coincide
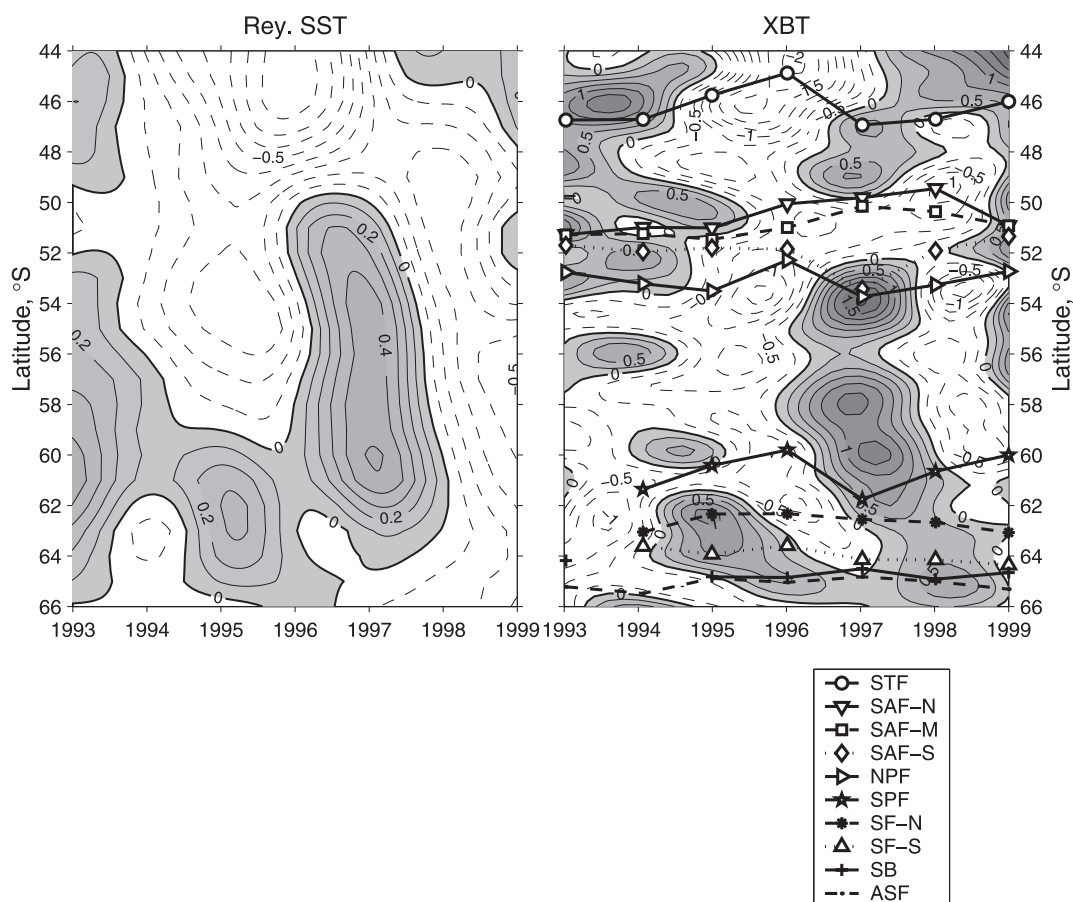
**Figure 4.** Long-period SST anomalies derived from continues Reynolds (left) SST data and from (right) XBT. Positive anomalies are indicated by shading.

with the locations of major fronts: near the southern branch of the PF at 60–61°S and the SF at 64°S. The higher correlations found near 56°S reflect the path of the PF-S in the vicinity of the XBT section. The PF-S first crosses the section at 60–61°S (Figure 1). As the front encounters the shoaling topography of the Southeast Indian Ridge, it is deflected equatorward, so the front runs more or less parallel to the section between 60 and 56°S. After crossing the ridge, the front shifts back to the south, completing the S-shaped turn, and continues to the east. The mean temperature field shown in the top panel of Figure 6 reflects the path of the PF-S: changes in thickness of the subsurface temperature maximum layer indicated by the 2.22°C contour coincide with changes of the PF-S position relative to the section.

[21] Figure 6 shows that temperature anomalies at depth are significantly correlated with SST anomalies in the vicinity of each of the major fronts. This suggests that meridional shifts of the fronts are the dominant driver of temperature anomalies in this region. The depth range over which the correlations extend depends on the temperature structure associated with each front. For example, the meridional temperature gradients associated with the STF are limited to the upper 400 m and likewise significant correlations are also found only in the upper 400 m. The ACC fronts extend throughout the water column, and the high correlations between surface and subsurface anomalies

are found throughout the upper 700 m at the SAF, PF-N, and SF/SB. At the PF-S, high correlations are found in the surface mixed layer and below the UCDW; as mentioned above, the lack of meridional temperature gradients in the WW and upper part of the UCDW means that meridional translations of the PF-S do not result in temperature anomalies in this depth range.

[22] Surface and subsurface anomalies are also highly correlated in the Subantarctic zone (46° to 51°S), where deep convection in winter homogenizes the upper 600 m of the water column. The high correlation between temperature anomalies in the summer mixed layer and those in the underlying remnant winter mixed layer suggests a cool winter preconditions the water column for cool conditions in the following summer. This is the only latitude band where the correlation between surface and subsurface temperature anomalies can be attributed to direct exchange with the atmosphere. (As noted above, the ''hole'' in the correlation pattern near 49°S reflects the presence or absence of a cold core ring that dominates the interannual variability at depth, but has little signature in the surface layer.) The other correlation maxima observed at depth extend below the depth of the winter mixed layer, and so are not in communication with the atmosphere during the annual cycle.

[23] The hypothesis that displacements of the fronts are responsible for the observed temperature anomalies is further supported by Figure 4. Negative (positive) SST
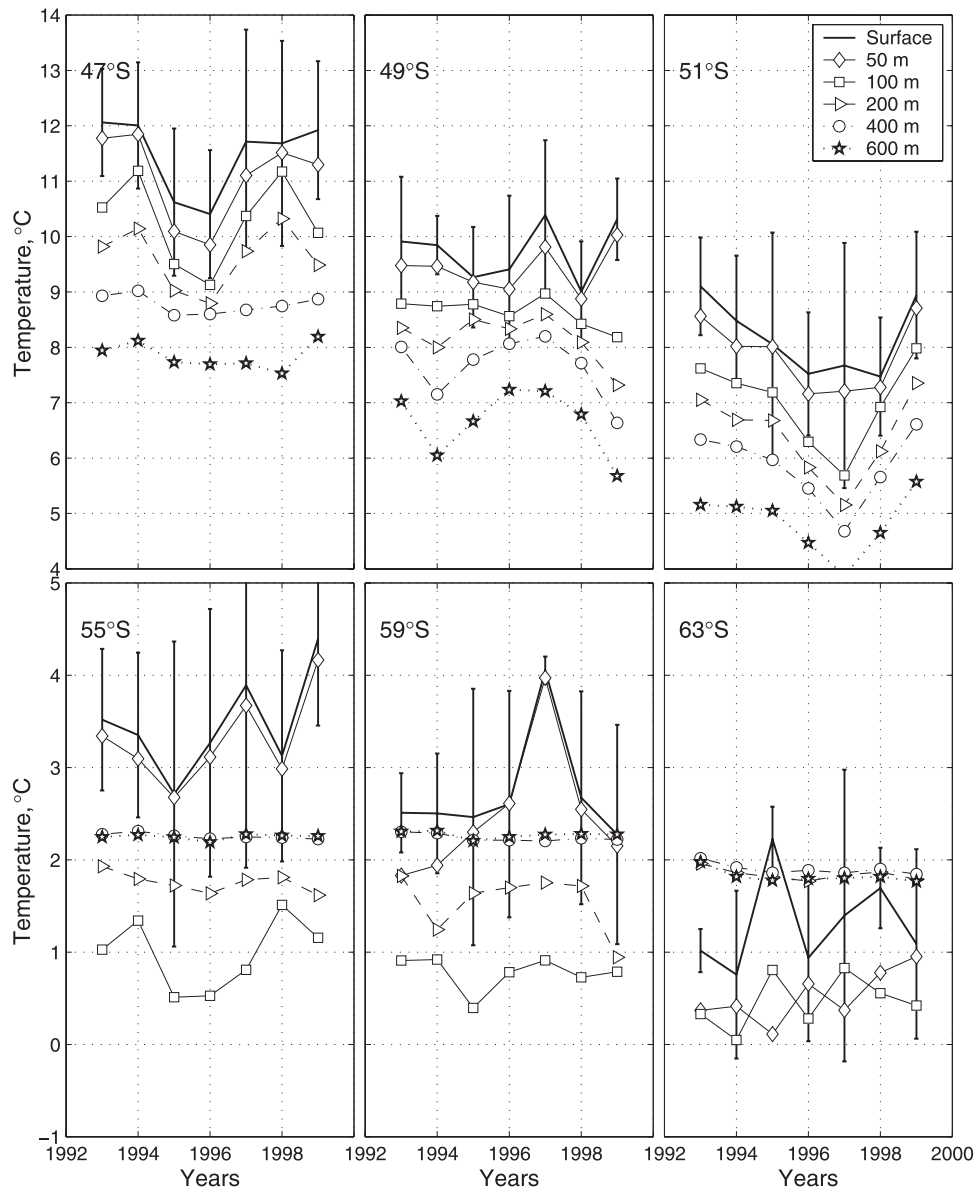
**Figure 5.** Vertical structure of interannual temperature changes across the SURVOSTRAL section. Casts within a 2° latitude band have been averaged for each austral summer. Temperature at six depths is shown (see legend). Standard deviations of sea surface XBT temperature estimated for each austral summer are indicated by vertical bars.

anomalies generally coincide with northward (southward) deviations of the fronts from their mean position. While the meridional displacements are relatively modest (1 to 2° of latitude), the SST gradients associated with the fronts are as large as 3°C/° latitude and small meridional shifts can result in significant SST anomalies. The large positive anomaly in 1997 near 58°S is not clearly related to a particular front. However, as noted above, the PF-S runs roughly from south to north along the section in this latitude band and the temperature anomaly may reflect zonal shifts of the meridional portion of the PF-S.

### 3.3. Low-Frequency Variability

[24] The XBT temperature changes discussed so far have included variations in both the interannual band (periods of 2–7 years) and longer period signals. While the XBT record is too short and discontinuous to allow these signals to be distinguished, the satellite-based SST record can be filtered to examine the relative contribution of different frequency bands (Figure 7).

[25] The spectrum of SST along the XBT line is shown in Figure 8. The strongest peaks are at semiannual and annual periods, as expected. The semiannual peak is larger south of 52°S, while the annual cycle is of roughly the same magnitude across the full width of the section. A broad peak at periods of 3 to 4 years, the signal of the ACW, is somewhat stronger north of 54°S than to the south. There is significant energy at periods of a decade and longer, but these periods are not resolved by the 17 year SST data set.

[26] The interannual signal along the section is highly regular with a nominal 4 year period (the ACW), but the amplitude of the signal in the 1990s is about 2–3 times
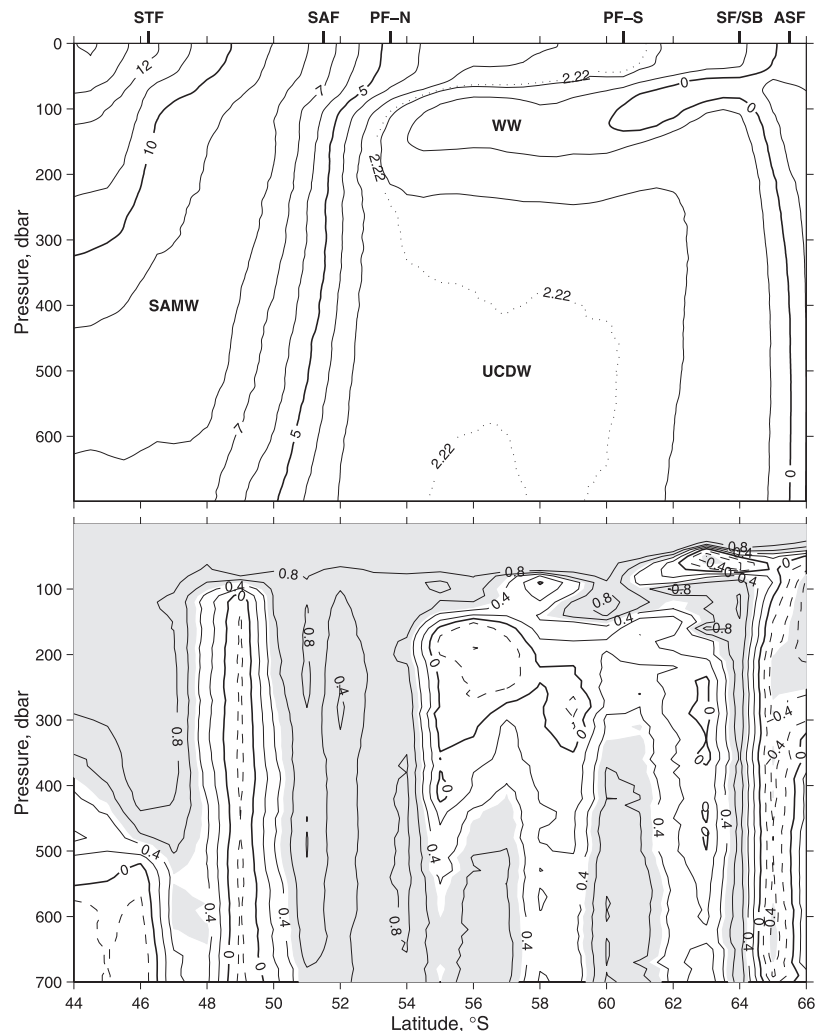
**Figure 6.** (top) Mean section of temperature (°C) and (bottom) vertical correlation between temperature changes at the surface and in the deeper layers. The location of major fronts and water masses are shown in the top panel. Shading in the bottom panel indicates correlations higher than 80% confidence level (the 80% confidence level for correlation is 0.48).

smaller than in the 1980s (Figure 7a). The south-north phase lag varies from 1 to 2 years, with changes in the south generally leading those in the north. The dominant period of the "quasi-decadal" (period >7 years) variations appears to be shorter near the northern end of the section than near Antarctica, but the period of both signals is comparable to the duration of the observations and so not resolved (Figure 7b). The amplitude of the "quasi-decadal" and interannual signals is comparable (meridional mean standard deviations of 0.19°C and 0.25°C, respectively). While the band-passed SST on the SURVOSTRAL line is similar in period and phase to the ACW described by *White and Peterson* [1996], the significant lower frequency anomalies alter the total signal with periods >2 years.

[27] A similar long period signal was detected using XBT measurements in the Indian sector of the Southern Ocean south of 60°S by *Aoki* [1997]. He found that the temperature at depths of 200–400 m rose by about 0.5°C between 1983 and 1994. This "trend" in the central Indian Ocean is similar in magnitude and phase to the "quasi-decadal" changes in SST at 60°S on the SURVOSTRAL section

(Figure 7b). *Aoki et al.* [2003] extended the earlier analysis to cover the period to 1998 and depths down to 1000 m. These authors found that the temperature tendency in the Indian Ocean reversed after 1994, as also seen at the SURVOSTRAL section (Figure 7b). *Aoki et al.* [2003] also noted that the amplitude of the temperature rise increased with depth between 200 and 1000 m, but did not offer an explanation of this observation. If temperature anomalies primarily reflect displacements of fronts, as argued here, we would expect the signal to increase with depth in this latitude band because the horizontal and vertical temperature gradients are very small between 200 and 400 m. At greater depth, the temperature gradients increase and a larger temperature anomaly results from a given meridional translation of the temperature field.

## 4. Conclusions

[28] We have used a 7 year time series of XBT sections to explore the vertical structure of Southern Ocean temperature anomalies. We find significant correlations between changes
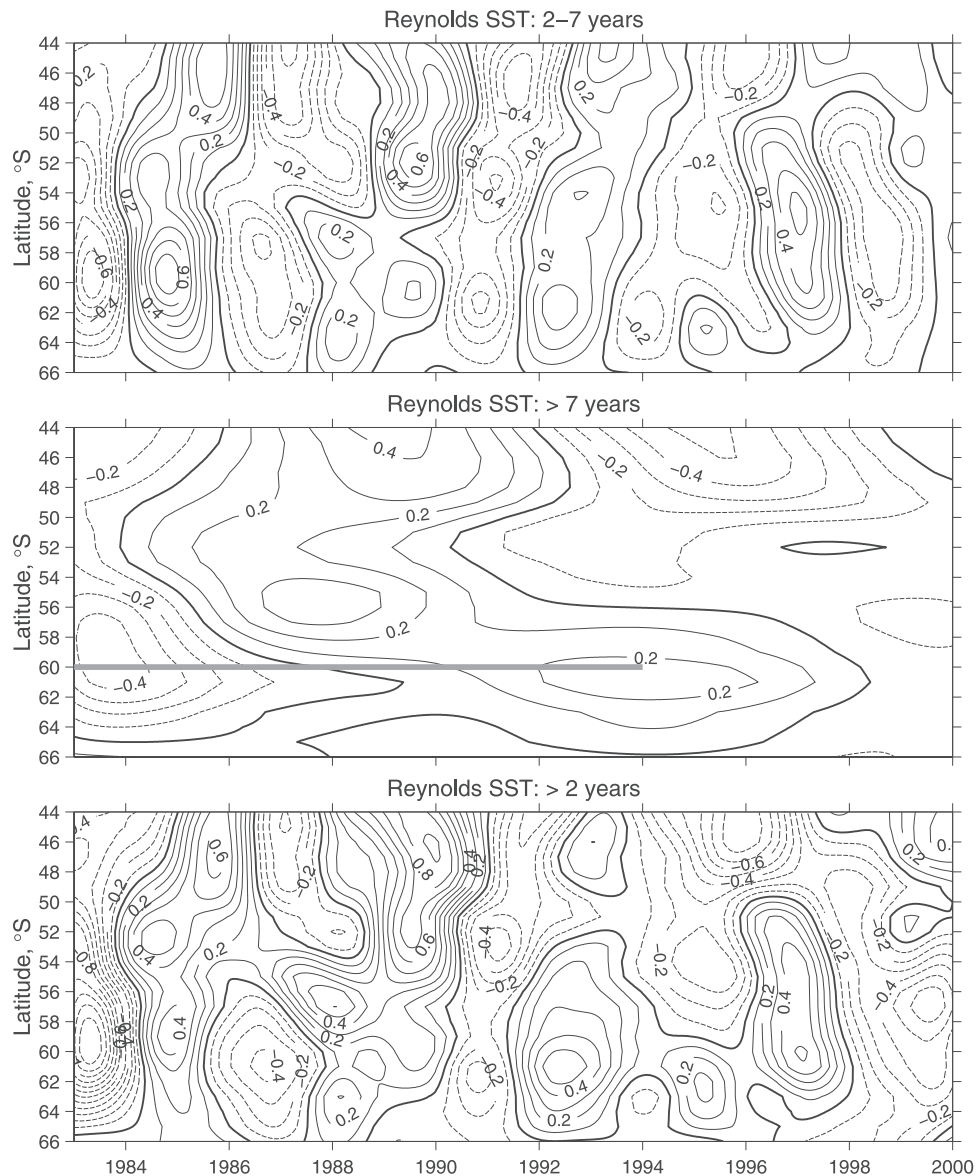
**Figure 7.** Long-period variation of SST (°C) for the SURVOSTRAL section: (top) the interannual signal (periods of 2–7 years), (middle) the "decadal" variability (periods longer than 7 years), and (bottom) the total long-period variations (periods longer than 2 years). Also, period of "decadal" changes in SST described by *Aoki* [1997] is shown in middle panel.

in surface and subsurface temperature across the width of the Southern Ocean. In particular, temperature changes are coherent throughout much of the upper 800 m near each of the major fronts and within the thick pool of SAMW. With the exception of the SAZ, parts of the section where the temperature gradients are small are characterized by low correlation between surface and subsurface temperature changes. Interannual SST anomalies have been shown to be related to meridional displacements of the major fronts, with equatorward shifts resulting in negative anomalies, and vice versa.

[29] Meridional shifts of the ACC fronts occur at a range of timescales and are likely driven by a variety of processes. For example, *Rintoul et al.* [2002] showed that SSH variability near the SAF was of roughly equal magnitude at mesoscale (periods less than 4 months), quasi-annual and

interannual periods (with standard deviations of 8.5–10 cm in each band). At short periods, the movement of the fronts is likely to be dominated by internal dynamical processes such as baroclinic instability of the ACC [e.g., *Phillips and Rintoul*, 2002]. At longer periods, local or remote forcing is likely to play a role. From the linear vorticity balance we expect variations in wind stress curl will drive meridional displacements of fluid columns and hence fronts. *Rintoul et al.* [2002] found that south of Australia at the WOCE SR3 line both wind stress and wind stress curl over a broad span of latitudes are correlated with variations in deep (2500 dbar) net baroclinic transport at interannual timescales, consistent with the idea that the upper ocean density field responds to changes in wind-forcing. The extent to which the deep-reaching fronts of the ACC can translate meridionally in response to forcing is also regulated by
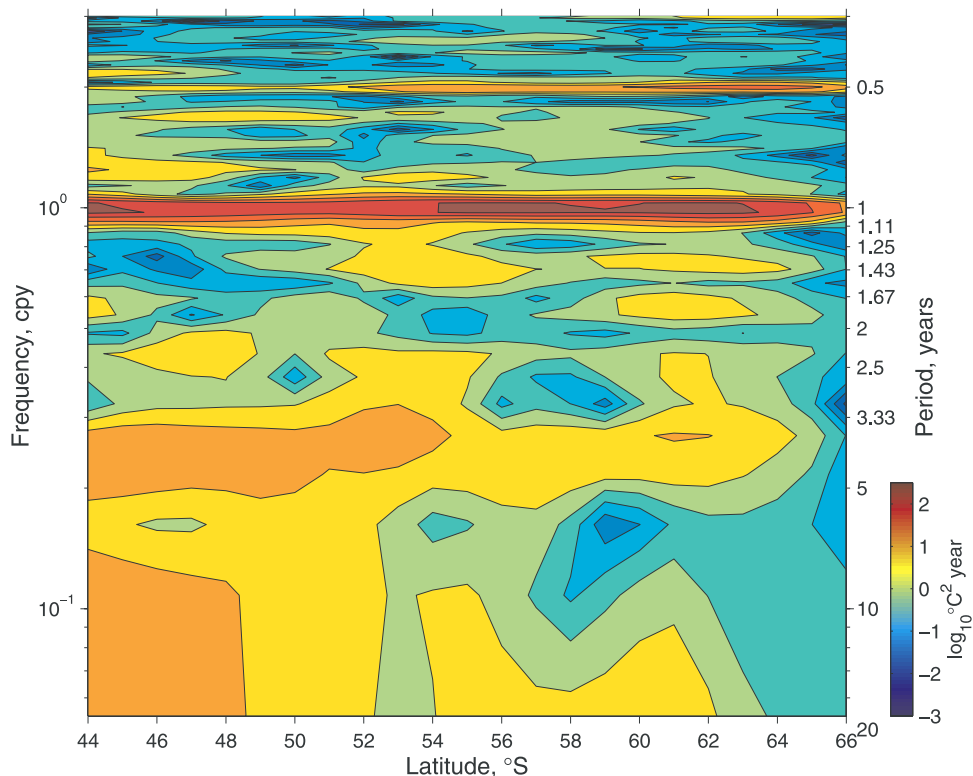
**Figure 8.**   Power spectrum of SST along the SURVOSTRAL line.

interaction with bathymetry, with less (more) variability observed near steep (flat) topography [*Sokolov and Rintoul*, 2002]. The variety of processes capable of driving translations of the fronts and the short XBT time series make it difficult to quantify the connection between wind-forcing and frontal shifts and temperature anomalies.

[30]   We anticipate that since the ACC fronts extend from the surface to the seafloor [*Rintoul and Sokolov*, 2001], similar temperature anomalies associated with frontal shifts would be found below 700 m depth as well. The large amplitude (0.1 m, [*Rintoul et al.*, 2002]) of interannual variations in SSH observed at the SAF supports the view that frontal shifts are vertically coherent throughout the water column. (For comparison, a 1°C temperature anomaly in a 100 m thick mixed layer changes the SSH by only 0.01 m, an order of magnitude smaller than the SSH variability in the frontal zones.)

[31]   This is the first attempt to estimate the vertical structure of interannual temperature anomalies across the full width of the Southern Ocean using in situ data. While our conclusions are based on observations from a single longitude, the circumpolar nature of Southern Ocean fronts suggests the results are likely to hold for the Southern Ocean as a whole. Therefore this study has implications for attempts to understand the dynamics of temperature anomalies in the Southern Ocean, as well as perhaps other regions of the World Ocean where significant fronts occur. For example, the temperature anomalies associated with the ACW are often interpreted as surface-trapped features advected eastward by the ACC. Our results show that Southern Ocean temperature anomalies in fact extend to depth. The main driving factors for such anomalies are

likely to be processes capable of causing shifts of fronts (e.g., wind stress curl anomalies rather than air-sea heat flux anomalies). Models of Southern Ocean phenomena which involve SST anomalies (e.g., the ACW) may need to resolve the frontal structure of the ACC if the simulations are to capture the fundamental dynamics. Coarse resolution models in which the fronts are unrealistically broad and weak may underestimate the SST response to changes in wind-forcing, and hence the potential for feedback on the atmosphere. More definitive conclusions regarding the link between wind-forcing, frontal shifts, and temperature anomalies will require longer time series of subsurface temperature observations from this and other Southern Ocean locations.

## References

Aoki, S., Trends and interannual variability of surface layer temperature in the Indian sector of the Southern Ocean observed by Japanese Antarctic research expeditions, *J. Oceanogr.*, *53*, 623–631, 1997.

Aoki, S., M. Yoritaka, and A. Masuyama, Multidecadal warming of subsurface temperature in the Indian sector of the Southern Ocean, *J. Geophys. Res.*, *108*(C4), 8081, doi:10.1029/2000JC000307, 2003.

Baines, P. G., and W. Cai, Analysis of an interactive instability mechanism for the Antarctic Circumpolar Wave, *J. Clim.*, *13*, 1831–1844, 2000.

Bindoff, N. L., and T. J. McDougall, Decadal changes along an Indian Ocean Section at 32°S and their interpretation, *J. Phys. Oceanogr.*, *30*, 1207–1222, 2000.

Bonekamp, H., A. Sterl, and G. J. Komen, Interannual variability in the Southern Ocean from an ocean model forced by European Center for Medium-Range Weather Forecasts reanalysis fluxes, *J. Geophys. Res.*, *104*, 13,317–13,331, 1999.

Christoph, M., T. P. Barnett, and E. Roeckner, The Antarctic Circumpolar Wave in a coupled ocean-atmosphere model, *J. Clim.*, *11*, 1659–1672, 1998.

Gille, S. T., Warming of the Southern Ocean since the 1950s, *Science*, *295*, 1275–1277, 2002.

Goodman, J., and J. Marshall, A model of decadal middle-latitude atmosphere-ocean coupled modes, *J. Clim.*, *12*, 621–641, 1999.

Meehl, G. A., J. W. Hurrell, and H. VanLoon, A modulation of the mechanism of the semiannual oscillation in the Southern Hemisphere, *Tellus, Ser. A*, *50*, 442–450, 1998.

Olbers, D., V. Gouretski, G. Seiß, and J. Schröter, *Hydrographic Atlas of the Southern Ocean*, Alfred Wegener Inst. for Polar and Mar. Res., Bremerhaven, Germany, 1992.

Peterson, R. G., and W. B. White, Slow oceanic teleconnections linking the Antarctic Circumpolar Wave with tropical ENSO, *J. Geophys. Res.*, *103*, 24,573–24,583, 1998.

Phillips, H. E., and S. R. Rintoul, A mean synoptic view of the Subantarctic Front south of Australia, *J. Phys. Oceanogr.*, *32*, 1536–1553, 2002.

Qiu, B., and F.-F. Jin, Antarctic circumpolar wave: An indication of ocean-atmosphere coupling in the extratropics, *Geophys. Res. Lett.*, *24*, 2585–2588, 1997.

Reynolds, R. W., and D. C. Marsico, An improved real-time global sea surface temperature analysis, *J. Clim.*, *6*, 114–119, 1993.

Rintoul, S. R., and S. Sokolov, Baroclinic transport variability of the Antarctic Circumpolar Current south of Australia (WOCE repeat section SR3), *J. Geophys. Res.*, *106*, 2795–2814, 2001.

Rintoul, S. R., J.-R. Donguy, and D. H. Roemmich, Seasonal evolution of upper ocean thermal structure between Tasmania and Antarctica, *Deep Sea Res.*, *44*, 1185–1202, 1997.

Rintoul, S. R., S. Sokolov, and J. Church, A 6 year record of baroclinic transport variability of the Antarctic Circumpolar Current at 140E derived from expendable bathythermograph and altimeter measurements, *J. Geophys. Res.*, *107*(C10), 3155, doi:10.1029/2001JC000787, 2002.

Sokolov, S., and S. R. Rintoul, Structure of Southern Ocean fronts at 140°E, *J. Mar. Sys.*, *37*, 151–184, 2002.

Talley, L. D., Simple coupled midlatitude climate models, *J. Phys. Oceanogr.*, *29*, 2016–2037, 1999.

Thompson, D. W. J., J. M. Wallace, and G. C. Hegerl, Annular modes in the extratropical circulation, part II: Trends, *J. Clim.*, *13*, 1018–1036, 2000.

Walker, A. E., and J. L. Wilkin, Optimal averaging of NOAA/NASA Pathfinder satellite sea surface temperature data, *J. Geophys. Res.*, *103*, 12,869–12,883, 1998.

Weisse, R., U. Mikolajewicz, A. Sterl, and S. S. Drijfhout, Stochastically forced variability in the Antarctic Circumpolar Current, *J. Geophys. Res.*, *104*, 11,049–11,064, 1999.

White, W. B., Influence of the Antarctic Circumpolar Wave on Australia precipitation from 1958–1996, *J. Clim.*, *13*, 2125–2141, 2000.

White, W. B., and N. J. Cherry, Influence of the Antarctic Circumpolar Wave upon New Zealand temperature and precipitation during autumn-winter, *J. Clim.*, *12*, 960–976, 1998.

White, W. B., and R. Peterson, An Antarctic Circumpolar Wave in surface pressure, wind, temperature and sea ice extent, *Nature*, *380*, 699–702, 1996.

White, W. B., S. C. Chen, and R. Peterson, The Antarctic Circumpolar Wave: A beta-effect in ocean-atmosphere coupling over the Southern Ocean, *J. Phys. Oceanogr.*, *28*, 2345–2361, 1998.

Yuan, X., and D. G. Martinson, Antarctic sea ice extent variability and its global connectivity, *J. Clim.*, *13*, 1697–1717, 2000.

————————————

S. R. Rintoul and S. Sokolov, CSIRO Marine Research and Antarctic CRC, GPO Box 1538, Hobart, Tasmania, Australia. (steve.rintoul@marine.csiro.au; serguei.sokolov@marine.csiro.au)